2013 IEEE International Conference on Robotics and Automation (ICRA)
Karlsruhe, Germany, May 6-10, 2013

Sampling-based Optimal Motion Planning for Non-holonomic Dynamical Systems

Sertac Karaman Emilio Frazzoli

Abstract— **Sampling-based motion planning algorithms, such as the Probabilistic RoadMap (PRM) and the Rapidly-exploring Random Tree (RRT), have received a large and growing amount of attention during the past decade. Most recently, sampling-based algorithms, such as the PRM* and RRT*, that guarantee asymptotic optimality, i.e., almost-sure convergence towards optimal solutions, have been proposed. Despite the experimental success of asymptotically-optimal sampling-based algorithms, their extensions to handle complex non-holonomic dynamical systems remains largely an open problem. In this paper, with the help of results from differential geometry, we extend the RRT* algorithm to handle a large class of non-holonomic dynamical systems. We demonstrate the performance of the algorithm in computational experiments involving the Dubins' car dynamics.**

I. Introduction

The motion planning problem, i.e., finding a trajectory from an initial state to a goal state in a complex environment, is a fundamental problem of robotics [1] with many applications well outside the robotics domain [2].

Despite the discouraging computational complexity results [3], many practical algorithms were proposed. In particular, algorithms based on sampling, such as the Probabilistic RoadMap (PRM) [4] and the Rapidly-exploring Random Tree (RRT) [5] algorithms, have achieved substantial experimental success (see, e.g., [6]). Often implemented using random sampling, these algorithms guarantee *probabilistic completeness*, i.e., the algorithm returns a feasible path, when one exists, with probability approaching to one as the number of samples approaches infinity [4], [5], [1].

In many applications of robotics, however, the quality of the solution returned by the algorithm is also a major concern. In fact, in the context of sampling-based motion planning, the importance of the quality of the motion, measured with respect to a cost function, has been realized early on [7], [8]. However, most existing algorithms relied on problem-specific heuristics and failed to provide any guarantees on convergence towards optimal solutions.

Recently, in our previous work in [9], we have studied sampling-based algorithms in terms of their convergence to optimal solutions. In particular, we have shown that, some of the widely-used path planning algorithms, such as the RRT, fail to converge to optimal solutions, with probability one. Subsequently, we have proposed two novel algorithms, called the PRM* and the RRT*, which guarantee *asymptotic optimality*, i.e., almost-sure convergence to globally optimal solutions, without sacrificing computational efficiency. In fact, the asymptotic computational complexity of these algorithms is the same as the most efficient existing sampling-based algorithms, such as the RRT. The enabling idea behind PRM* and RRT* algorithms is to connect samples within hyperspheres of volume $\log n/n$, a rate that guarantees asymptotic optimality and computational efficiency at the same time. More recently, the RRT* algorithm was demonstrated on a number of robotic platforms [10], [11].

In [9], we have focused solely on holonomic dynamical systems (in the sense defined later in this paper). In this paper, we propose modifications to the PRM* and RRT* algorithms in order to handle a large class of non-holonomic dynamical systems. In particular, we show that, by seeking connections within boxes that are substantially larger in some dimensions than others, both asymptotic optimality and computational efficiency can be ensured. The shape and orientation of these boxes can be efficiently computed for a large class of dynamical systems. Our analysis is based on differential geometry, and it provides new insight into sampling-based algorithms tailored for planning problems involving non-holonomic dynamical systems, which may be of independent interest. In particular, our results may also lead to effective nearest neighbor search metrics for RRTs.

Our work in this paper extends our previous work in [12], where we had identified an RRT* variant for a class of non-holonomic dynamical systems. Although this variant was asymptotically optimal, it was not as efficient as, for example, the RRT algorithm. Extending RRT* to deal with non-holonomic dynamical systems have also been considered by many others (see, e.g., [13], [14]). Most of this very recent research focuses on developing steering functions for various classes of dynamical systems. In contrast, our work in this paper is on ensuring computational effectiveness of the algorithm, when the steering function is given.

II. Problem Definition

Consider the following time-invariant dynamical system:

$$\dot{x}(t) = f(x(t), u(t)), \qquad x(0) = x_0 \tag{1}$$

where $x(t) \in X \subseteq \mathbb{R}^n$, $u(t) \in U \subseteq \mathbb{R}^m$, $f : X \times U \to \mathbb{R}^n$ is Lipschitz continuous in both of its arguments.[1]

The state $x_0 \in X$ (see Equation (1)) is called the *initial state*. Let $X_{\text{obs}} \subset X$ and $X_{\text{goal}} \subset X$, called the *obstacle set* and the *goal set*, be open relative to X. Let $c : \Sigma \to \mathbb{R}_{\geq 0}$ be a *cost function* that assigns to each non-trivial trajectory

The authors are with the Department of Aeronautics and Astronautics, Massachusetts Institute of Technology. Email: sertac,frazzoli@mit.edu

[1]We tacitly assume that the sets X and U are smooth manifolds (see Section III-A for the definition of a smooth manifold).

978-1-4673-5643-5/13/$31.00 ©2013 IEEE

a non-zero cost. Then, the *motion planning problem* is to find a dynamically-feasible trajectory $x : [0, T] \to X$ that (i) starts from the initial state, i.e., $x(0) = x_0$, (ii) avoids collision with obstacles, i.e., $x(t) \notin X_{\text{obs}}$ for all $t \in [0, T]$, and (iii) reaches the goal region, i.e., $x(T) \in X_{\text{goal}}$. The *optimal motion planning problem* is to find a trajectory $x^* : [0, T] \to X$ that solves the motion planning problem while minimizing the cost function c.

III. The Shape of Small-time Attainable Sets

Given a state $x_0 \in X$ and a real number $t > 0$, define the *small-time attainable set*, denoted by $\mathcal{A}(x_0, t)$, as the set of all states reachable within time t by the dynamical system described by Equation (1) when the system starts from the state x_0. The *attainable set* is defined as $\mathcal{A}(x_0) := \bigcup_{t>0} \mathcal{A}(x_0, t)$. The following property, also called the *accessibility property* by D. Elliot [15], will play an important role in our analysis.

Definition 1 *A system is said to be* small-time locally attainable *(STLA) at state $x_0 \in X$ if $\mathcal{A}(x_0, t)$ has a non-empty interior (with respect to X) for all $t > 0$.*

It is worth noting at this point that the small-time attainability property is closely related to small-time local controllability. According to Sussmann [15], a system described by Equation (1) is said to be *small-time locally controllable* (STLC) at $x_0 \in X$ if $\mathcal{A}(x_0, t)$ contains a neighborhood of x_0 for all $t > 0$ and *locally controllable* at x_0 if $\mathcal{A}(x_0)$ contains an open neighborhood of x_0. Clearly, the STLC property implies the STLA property. Hence, STLC is a stronger condition. For instance, the Dubins' car [16] is STLA but not STLC [17]. In Section III-C, we recall the conditions under which a system is STLA or STLC.

In rest of this section, a key lemma characterizing the small-time attainable set for a large class of dynamical systems is provided (see Lemma 4). This key lemma constitutes the building block for the proposed algorithms in Section IV and for our analysis to follow in Section V.

Before stating this result, some other useful results from sub-Riemannian geometry are introduced in this section. Along the way, a number of examples from control theory and robotics are provided. Our notation in this section is fairly standard and closely follows that of Montgomery [18]. For a detailed exposition to sub-Riemannian geometry, the reader is referred to the monographs [19], [20], [18], [21].

A. Fundamentals of Differential Geometry

Let $n, m \in \mathbb{N}$, and let $V \subseteq \mathbb{R}^n$ and $W \subseteq \mathbb{R}^m$ be open sets. Recall that a function $f : V \to W$ is said to be *smooth* if all its partial derivatives exist and are continuous. The function f is said to be a *diffeomorphism* if f is a bijection and both f and its inverse f^{-1} are smooth. Two open sets V, W are said to be *diffeomorphic* if there exists such a diffeomorphism.

A set $M \subseteq \mathbb{R}^n$ is a *smooth d-dimensional manifold*, if, for all $p \in M$, there exists an open set $V \subset \mathbb{R}^n$ such that $V \cap M$ is diffeomorphic to an open set $V' \subset \mathbb{R}^d$.[2] An *interval*, usually denoted by I, is a convex subset of $\mathbb{R}$. A *smooth curve* on a manifold M is a smooth function $\gamma : I \to M$ for some interval I that includes the origin. Given a point $p \in M$, a vector $v \in \mathbb{R}^n$ is said to be a *tangent vector* of M at p, if there exists a smooth curve $\gamma : \mathbb{R} \to M$ such that $\gamma(0) = p$ and $\dot{\gamma}(0) = v$. The *tangent space* of M at p is defined as $T_pM := \{\dot{\gamma}(0) \,|\, \gamma \text{ is a smooth curve on } M \text{ and } \gamma(0) = p\}$.

Example A trivial example of a manifold is the n-dimensional Euclidean space, $\mathbb{R}^n$, which is n-dimensional, since it is diffeomorphic to itself. One of the most basic examples of a non-trivial manifold is the unit circle. Defined as $S^1 := \{(x_1, x_2) \in \mathbb{R}^n \,|\, \sqrt{x_1^2 + x_2^2} = 1\} \subset \mathbb{R}^2$, it is a one-dimensional manifold that has important applications in robotics [23], [1]. In particular, the configuration space of an n-link planar manipulator can be represented by its n joint angles, hence the manifold formed by the Cartesian product of n unit circles, i.e., $S^1 \times S^1 \times \cdots \times S^1$. Another example is the configuration space of a Reeds-Shepp car [24] involving its planar position and its orientation, i.e., $\mathbb{R}^2 \times S^1$. ■

B. Sub-Riemannian Geometry

A smooth function $Y : M \to \mathbb{R}^n$ is said to be a *smooth vector field* on the manifold M, if $Y(p) \in T_pM$ for all $p \in M$. The set of all smooth vector fields on M is denoted by $\text{VF}(M)$. Let $k, l \in \mathbb{N}$. A set $E \subset M \times \mathbb{R}^l$ is said to be a *smooth vector bundle* of rank k over the manifold M, if the set $E_p := \{v \in \mathbb{R}^l \,|\, (p, v) \in E\}$ is a k-dimensional linear subspace of $\mathbb{R}^l$. The set E_p is also called the *fiber* of E over p. In particular, the vector bundle $TM := \{(p, v) \,|\, p \in M, v \in T_pM\}$ is called the *tangent bundle* of M. Note that its fiber, T_pM, is an m-dimensional linear subspace of $\mathbb{R}^n$. A *subbundle* of a vector bundle is a subset that is a vector bundle on its own right.

A *distribution* on a manifold M is a subbundle $\mathcal{H}$ of the tangent bundle TM. A *sub-Riemannian geometry* on a manifold M is a distribution $\mathcal{H}$ on M together with an inner product $\langle \cdot, \cdot \rangle : \mathcal{H} \times \mathcal{H} \to \mathbb{R}_{\geq 0}$. The set $\mathcal{H}$ is also called the *horizontal distribution*. The fiber of $\mathcal{H}$ at a point $p \in M$ is denoted by $\mathcal{H}_p$. A curve $\gamma : I \to M$ defined on the manifold M is said to be *horizontal* if it is tangent to $\mathcal{H}$, i.e., $\dot{\gamma}(t) = \mathcal{H}_{\gamma(t)}$ for all $t \in I$.

Example Suppose the configuration space of a robot is represented by a manifold M. Then, the dynamics governing this robot, i.e., constraints on its velocities while moving within its configuration space, can be represented by a distribution. Recall from the previous example that the configuration space of the Reeds-Shepp car can be represented by the manifold $M = \mathbb{R}^2 \times S^1$ encoding its planar position and its orientation. To succinctly describe its dynamics, define the state variables (x, y, θ), where $(x, y) \in \mathbb{R}^2$ describes the position and $\theta \in [-\pi, \pi]$ describes orientation. Then, $\dot{x}(t) =$

[2] In general, a smooth manifold is a Hausdorff space with a countable basis such that any point on the manifold has a neighborhood that is diffeomorphic to an open subset of the Euclidean space [22]. For all practical purposes, we are only interested in manifolds that are subsets of an Euclidean space.

$u_1(t)\cos(\theta(t)), \dot{y}(t) = u_1(t)\sin(\theta(t)), \dot{\theta}(t) = u_1(t)\,u_2(t)$ where $|u_1(t)|, |u_2(t)| \leq 1$. The input signals u_1, u_2 denote the forward velocity and the steering angle, respectively.

Right hand side of the equation induces a distribution on the manifold M. At the origin, i.e., at $(x, y, \theta) = (0, 0, 0)$, this distribution is spanned by $(1, 0, 0)$ and $(0, 0, 1)$. These vectors span a two dimensional plane along the coordinates x and θ. This merely indicates that the car can move in the longitudinal direction and it can change its orientation; but it can not move sideways, as the vector $(0, 1, 0)$ is not included in the span of the distribution at the origin. ■

The length of a (smooth) horizontal curve γ is defined as $\text{Length}(\gamma) = \int_I \|\dot{\gamma}(t)\| dt$, where $\|\dot{\gamma}(t)\| = \sqrt{\langle\dot{\gamma}(t), \dot{\gamma}(t)\rangle}$. Since we are only interested in manifolds that are submanifolds of an Euclidean space, we will take the inner product to be the usual Euclidean inner product. Thus, $\|\cdot\|$ denotes the usual Euclidean norm on $\mathbb{R}^n$ throughout this paper. The length function induces a distance function on M. Given two points $p, p' \in M$, the *sub-Riemannian distance* from p to p' is defined as $d(p,p') := \inf\{\text{Length}(\gamma) \,|\, \gamma \text{ is a smooth horizontal curve that connects } p \text{ and } p'\}$. By convention, $d(p,p')$ is infinite if there is no such curve. Define the *sub-Riemannian ball* of radius ϵ centered at p as $B(p, \epsilon) := \{p' \in M \,|\, d(p, p') \leq \epsilon\}$.

Central to our analysis will be the size of the sub-Riemannian ball. In what follows, we recall from the differential geometry literature an important result, called the ball-box theorem, which provides an asymptotic estimate for the size of the sub-Riemannian ball (see Theorem 3). First, let us introduce some preliminary definitions.

Given two vector fields Y, Z defined on a smooth manifold M, their *Lie bracket* is a vector field defined as $[Y, Z](p) := dZ(p)Y(p) - dY(p)Z(p)$, for all $p \in M$, where $dY(p) : T_pM \to \mathbb{R}^n$ denotes the derivative of the Y at point $p \in M$. The derivative of Y at point $p \in M$ in direction $v \in T_pM$, denoted by $dY(p)\,v$, is defined as follows. Let $\gamma : \mathbb{R} \to M$ be a smooth curve such that $\gamma(0) = p$ and $\dot{\gamma}(0) = v$, and define $dY(p)\,v = \frac{d}{dt}\big|_{t=0} Y(\gamma(t)) = \lim_{s\to 0} \frac{Y(\gamma(s)) - Y(p)}{s}$.

Let $\text{Lie}(\mathcal{F})$ denote the set of all vector fields formed by $\mathcal{F}$ along with all iterated Lie brackets of vector fields from $\mathcal{F}$, i.e., $\text{Lie}(\mathcal{F}) := \mathcal{F} \cup \{[Y_1, [Y_2, \dots [Y_{n-1}, Y_n] \dots] \,|\, Y_i \in \mathcal{F}, n \in \mathbb{N}\}$. It can be shown that $\text{Lie}(\mathcal{F})$, also called the *Lie hull* of $\mathcal{F}$, is a Lie algebra. Given a manifold M and a point $p \in M$, define $\text{Lie}(\mathcal{F})_p := \{Y(p) \,|\, Y \in \text{Lie}(Y)\}$.

Given a distribution $\mathcal{H}$ on M, let $\mathcal{H}_p$ denote its fiber at the point $p \in M$. Define $\mathcal{H}^1 := \{Y \in \text{VF}(M) \,|\, Y(p) \in \mathcal{H}_p\}$. For all $k \in \mathbb{N}$ and $k > 1$, define $\mathcal{H}^{k+1} := \mathcal{H}^k \cup [\mathcal{H}^1, \mathcal{H}^k]$, where $[\mathcal{H}^1, \mathcal{H}^k] = \text{Span}\{[Y, Z] \,|\, Y \in \mathcal{H}^1, Z \in \mathcal{H}^k\}$. Define the fiber of $\mathcal{H}^k$ at point $p \in M$ as $\mathcal{H}^k_p := \{Y(p) \,|\, Y \in \mathcal{H}^k\}$. Then, the Lie hull of $\mathcal{H}$ is simply $\text{Lie}(\mathcal{H}) := \bigcup_{k\geq 1} \mathcal{H}^k$. Its fiber over $p \in M$ is $\text{Lie}(\mathcal{H})_p := \{Y(p) \,|\, Y \in \text{Lie}(\mathcal{H})\}$. The distribution $\mathcal{H}$ is said to be *bracket generating*, if the Lie hull of $\mathcal{H}$ spans the whole tangent space of M, i.e., $\text{Lie}(\mathcal{H})_p = T_pM$ for all $p \in M$. A central result in sub-Riemannian geometry is stated in the following theorem.

Theorem 2 (Chow's Theorem [25] (see [18])) *Let $\mathcal{H}$ be a bracket generating distribution on a connected manifold M. Then, any two points of M is joined with a horizontal path.*

The condition that "the distribution is bracket generating" is called Chow's condition in sub-Riemannian geometry [18], the linear algebra rank condition in control theory [26], [27], [28], and Hörmander's condition in the context of PDEs [29].

Example We continue the previous example. Given any configuration (x, y, θ) of the Reeds-Shepp car, the vector fields $Y_1 = (\cos\theta, \sin\theta, 0)$ and $Y_2 = (0, 0, 1)$ span the distribution induced by its dynamics. The Lie bracket of these two vector fields can be calculated as $[Y_1, Y_2] = (-\sin\theta, \cos\theta, 0)$. Notice that the vector fields $\{Y_1, Y_2, [Y_1, Y_2]\}$ span the whole tangent space, satisfying Chow's condition. Then, Chow's theorem merely tells us that, given two configurations of the Reeds-Shepp car, there exists a dynamically-feasible trajectory, i.e., a horizontal curve, that joins the two. ■

Let $\mathcal{H}$ be a bracket generating distribution. Then, for any $p \in \mathcal{H}$, there exists an integer $r(p)$ such that $\mathcal{H}_p \subset \mathcal{H}^2_p \subset \dots \subset \mathcal{H}^{r(p)}_p = T_pM$. The smallest such integer is called the *degree of nonholonomy* of the distribution $\mathcal{H}$ at point p [30], [18]. Define $n_k(p) := \dim(\mathcal{H}^k_p)$. Then, $(n_1(p), n_2(p), \dots, n_{r(p)}(p))$ is called the *growth vector* of $\mathcal{H}$ at p. Note that, when $\mathcal{H}$ is bracket generating, the dimensionality of $\mathcal{H}^{r(p)}_p$ equals to that of T_pM, i.e., $n_{r(p)} = n$. The point p is called a *regular point* if there exists an open neighborhood of M around p such that the growth vector is constant; otherwise, p is said to be a *singular point* of $\mathcal{H}$.

For a given vector field Y, let $\exp tY$ denote its flow. That is, $(\exp tY) : M \to M$ is such that $(\exp tY)(p)$ is equal to $y(t)$ where $y : [0, t] \to M$ is a solution to the following differential equation: $\frac{d}{dt} y(\tau) = Y(y(\tau))$ and $y(0) = p$. In other words, $(\exp tY)(p)$ denotes the point that a system evolving on the manifold M reaches under the influence of the vector field Y for t time units starting from the point p.

Suppose that p is a regular point, and denote the growth vector simply as $(n_1, n_2, \dots, n_r)$, where $n_r = n$. Define the vector fields $Y_1, Y_2, \dots, Y_n$ as follows: the set $\{Y_1, Y_2, \dots, Y_{n_1}\}$ of vector fields spans $\mathcal{H}$; the set $\{Y_1, Y_2, \dots, Y_{n_2}\}$ spans $\mathcal{H}^2$; and so on. Define the joint flow of all these vector fields as $\Phi(t_1, t_2, \dots, t_n; p) := \big((\exp t_1 Y_1) \circ (\exp t_2 Y_2) \circ \dots \circ (\exp t_n Y_n)\big)(p)$, where $\circ$ denotes the functional composition operator. Hence, $\Phi(t_1, t_2, \dots, t_n; p)$ denotes the point reached under the influence of vector field Y_n for t_n time units, then Y_{n-1} for t_{n-1} time units, and so on. Since p is a regular point, such a map can be defined in some neighborhood of p. For notational convenience, define the weights $w_i := k$ if $Y_i(p) \in \mathcal{H}^k_p$ and $Y_i(p) \notin \mathcal{H}^{k+1}_p$ for all $i \in \{1, 2, \dots, n\}$, and define $w := (w_1, w_2, \dots, w_n)$. Finally, define the *$w$-weighted box* of size $\epsilon > 0$ centered at $p \in M$ as

$$\text{Box}^w(p, \epsilon) := \{\Phi(t_1, t_2, \dots, t_n; p) \,|\, |t_k| \leq \epsilon^{w_k}\}.$$

Recall that the *sub-Riemannian ball* of radius ϵ centered at p is defined as $B(p, \epsilon) := \{p' \in M \,|\, d(p, p') \leq \epsilon\}$.

The following theorem, attributed to Mitchell, Gershkovich, and Nagel-Stein-Wainger by Gromov [20], is of central importance for the purposes of this paper.

Theorem 3 (Ball-Box Theorem (see [18])) *Assume $\mathcal{H}$ satisfies Chow's condition. Then, there exists constants $\epsilon_0, c, C > 0$ such that for all $\epsilon < \epsilon_0$ and for all $p \in M$,*

$$\mathrm{Box}^w(p, c\epsilon) \subset B(p, \epsilon) \subset \mathrm{Box}^w(p, C\epsilon).$$

The ball-box theorem states that the set of states that can be reached by a horizontal path starting from p contains a weighted box of radius $c\,\epsilon$ and is contained in a box of radius $C\,\epsilon$. The orientation of these boxes at a particular point is determined by the vector fields $\{Y_1, Y_2, \ldots, Y_n\}$ evaluated at that point. It is remarkable that the shape of the sub-Riemannian ball can be estimated up to a constant factor for an arbitrary distribution. This result will be used in the next section to estimate the shape of the small-time attainable sets, which in turn will be used heavily in our analysis.

C. Links with Control Systems

It was recognized early on that Chow's theorem has implications on the attainability and controllability properties of dynamical systems. For example, Hermann [31] has shown that, for any real analytic system that is symmetric in the sense that any dynamically-feasible trajectory run backwards is also a dynamically-feasible trajectory, the system is controllable if and only if Chow's condition holds. In fact, the sufficiency of Chow's condition is immediate from Theorem 2. An example of such a system is a driftless control-affine real-analytic dynamical system with the property that the control set U is symmetric with respect to the origin.

In [30], the author studies such systems in depth using Lie theoretic methods. In particular, it is known that a symmetric real-analytic system is small-time locally controllable if and only if Chow's condition holds. Moreover, the ball box theorem provides distance estimates in the following sense. The dynamics can be written in the following form: $\dot{x}(t) = \sum_{i=1}^{m} u_i(t)\, g_i(x(t))$, where $x(t) \in M$ and $u(t) \in U$. Let $\mathcal{H}$ denote the distribution generated by g_i's. Suppose that $\mathcal{H}$ satisfies Chow's condition and $x_0 \in M$ is a regular point of $\mathcal{H}$. Denote the weight vector at x_0 by $w = (w_1, \ldots, w_n)$. Then, there exists $t_0, c, C > 0$ such that $\mathrm{Box}^w(x_0, ct) \subset \mathcal{A}(x_0, t) \subset \mathrm{Box}^w(x_0, Ct)$ for all $t < t_0$ [30].

It is can be shown that a symmetric real-analytic system is STLC if and only if it is STLA. Thus, for such systems, Chow's condition characterizes both the STLC and STLA properties in terms of Lie brackets. However, many realistic engineering systems are not symmetric. (Important examples include the class of linear systems and systems with drift.)

Fortunately, the small-time local attainability property is completely characterized in terms of Lie brackets by Krener [32] (see also [33]). His result, usually called the positive form of Chow's theorem [15], implies the following. Consider a real-analytic control-affine system: $\dot{x}(t) = f(x(t)) + \sum_{i=1}^{m} u_i(t)\, g(x(t))$. This system is STLA if and only if the distribution generated by $\{f, g_1 \ldots, g_m\}$ satisfies Chow's condition. Moreover, Krener's result can be related to the ball-box theorem as follows.

Lemma 4 *Let $\mathcal{H}$ denote the distribution (on M) that is generated by the vector fields $\{f, g_1, \ldots, g_m\}$. Suppose $\mathcal{H}$ satisfies the Chow's condition. Let x_0 be a regular point of this distribution. Let w denote the weight vector at x_0. Then, there exists constants $t_0, c > 0$ such that for all $t < t_0$ there exists a point $x_1 \in M$ such that $\mathrm{Box}^w(x_1, ct) \subset \mathcal{A}(x_0, t)$.*

This lemma will play a central role in proving our main results (Theorems 5 and 6). The proof of Lemma 4 follows from the results in [33], [32]. Below, we provide an example that illustrates Hermann's result and Lemma 4.

Example Denote the distribution induced by the dynamics of the Reeds-Shepp car by $\mathcal{H}$. From the previous example, $\mathcal{H} \subset \mathcal{H}^2 = T_pM$, and that the vector fields $Y_1 = (\cos\theta, \sin\theta, 0)$, $Y_2 = (0, 0, 1)$, and $Y_3 = (-\sin\theta, \cos\theta, 0)$ are such that $\mathrm{Span}\{Y_1, Y_2\} = \mathcal{H}$ while $\mathrm{Span}\{Y_1, Y_2, Y_3\} = \mathcal{H}^2$. Since $\dim(\mathcal{H}) = 2$ and $\dim(\mathcal{H}^2) = 3$, the growth vector is $(2, 3)$ for all points on the manifold describing the configuration space of the Reeds-Shepp car. The weight vector, on the other hand, can be computed as $w = (1, 2, 1)$.

Suppose that the car is at the origin, i.e., $(x, y, \theta) = \mathbf{0} := (0, 0, 0)$. Then, $Y_1(\mathbf{0}) = (1, 0, 0)$, $Y_2(\mathbf{0}) = (0, 0, 1)$, and $Y_3(\mathbf{0}) = (0, 1, 0)$. In this case, the ball-box theorem implies that the set of states reachable from $\mathbf{0}$ within t time units contains a box of size $[-ct, ct] \times [-ct^2, ct^2] \times [-ct, ct]$ for all small enough $t > 0$, where $c > 0$ is a constant.

That is, the car can move a distance of ct in the longitudinal direction within t time units, and it can turn with a constant speed, both of which are apparent from the equations describing its dynamics. However, the ball-box theorem also estimates that the car can move a distance of ct^2 towards the lateral direction by combining its maneuvers, which is not immediately obvious.

Let us explicitly provide a sequence of maneuvers that translates the car sideways for at least a distance of ct^2 within time t. Consider the following four maneuvers applied sequentially in this order: (i) forward and right, i.e., $u_1(t) = u_2(t) = -1$, (ii) forward and left, i.e., $u_1(t) = 1, u_2(t) = 1$, (iii) backward and right, i.e., $u_1(t) = -1, u_2(t) = -1$, and (iv) backward and left, i.e., $u_1(t) = -1, u(t) = 1$, with each set of controls applied $T/4$ time units. See Figures 1.(a)-(b).

As seen in the figure, with each maneuver the car moves a distance of $1 = \cos(\alpha) = 1 - \cos((\pi/2)\, t)$ along the y-axis. Using the Taylor expansion, $\cos\alpha = 1 - \frac{\alpha^2}{2!} + \frac{\alpha^4}{4!} - \cdots$, we conclude that total distance traveled by the car along the y-axis satisfies $4\,(1 - \cos((\pi/2)\, t)) = ct^2 + o(t^2)$. Hence, the car ends up roughly at the point $(0, ct^2, 0)$, confirming the result of the ball-box theorem. ■

Example An example of a dynamical system with drift is the Dubins' car [16] described by the following set of equations: $\dot{x}(t) = \cos(\theta(t)), \dot{y}(t) = \sin(\theta(t)), \dot{\theta}(t) = u(t)$ where $|u(t)| \leq 1$ is the steering input. In this model, the Dubins car travels with constant unit speed.

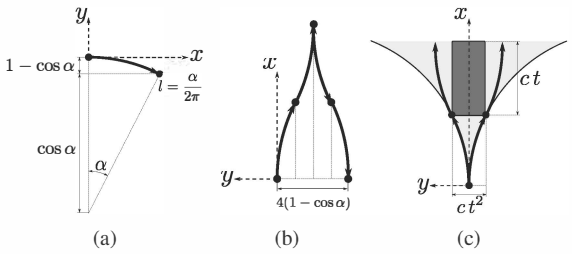

Fig. 1. Figure (a) shows the resulting trajectory of the vehicle when it moves forward while turning right. Figure (b) shows the resulting trajectory after four maneuvers. The x- and y-axes are also shown in the figures. In Figure (c), the small-time reachable set of the Dubins car and the box of size $[-ct, ct] \times [-ct^2, ct^2] \times [ct, ct]$ that is included in the reachable set are illustrated. Only the projection of these sets to x- and $y-$axes are shown. The projection of the reachable set is shaded in light grey whereas that of the box is shaded in dark grey.

By Lemma 4, the set of states reachable within time t starting from (x, y, θ) includes a box with size $[-ct, ct] \times [-ct^2, ct^2] \times [-ct, ct]$ oriented in coordinates $(\cos\theta, \sin\theta, 0)$, $(-\sin\theta, \cos\theta, 0)$, $(0, 0, 1)$. (Figure 1.(c).) ■

In the rest of this paper, we will focus on real analytic control-affine dynamical systems of the following form: $\dot{x}(t) = f(x(t)) + \sum_{i=1}^{m} u_i(t)\, g_i(x(t)), \quad x(0) = x_0$ where $x(t) \in X \subset \mathbb{R}^n$, $u(t) = (u_1(t), u_2(t), \ldots, u_m(t)) \in U$, $f(\cdot, \cdot)$ is a real analytic function, and X is a real analytic manifold. Let $\mathcal{H}$ denote the distribution generated by the vector fields $\{f, g_1, \ldots, g_m\}$. In the sequel, we refer to $\mathcal{H}$ as the distribution generated by the dynamics.

Recall that $\mathrm{Box}^w(x, \epsilon)$ denotes the weighted box of size ϵ centered at $x \in X$, where $w = (w_1, w_2, \ldots, w_n)$ denotes the weight vector at x. We assume that the weight vector is constant over the whole manifold X. Define $D := \sum_{i=1}^{n} w_i$. The integer D is at least as large as the dimensionality n of the state space. Let us note that D coincides with the Hausdorff dimension of the distribution $\mathcal{H}$ (see [18]).

IV. Algorithm

Before presenting the RRT* algorithm for non-holonomic dynamical systems, let us note the following primitive procedures. Recall that $\|\cdot\|$ denotes the usual Euclidean norm.

a) Sampling: The `Sample` procedure returns uniformly random samples from the free space on the maximal integral manifold of the dynamics through x_0, i.e., $N_{x_0} \setminus X_{\mathrm{obs}}$.

b) Local Steering: Given two states $x_1, x_2 \in X$, the `Steer` procedure returns a terminal time T and a dynamically-feasible trajectory connecting x_1 to x_2. This trajectory is denoted by $\texttt{Steer}(x_1, x_2) : [0, T] \to X$. We assume that the local steering procedure satisfies the *topological property* (see [17]), i.e., for any $\epsilon > 0$ there exists some real number $\eta_\epsilon > 0$ such that, for any two states $x_1, x_2 \in X$ with $\|x_1 - x_2\| < \eta$, we have $\|x_1 - \texttt{Steer}(x_1, x_2)(t)\| < \epsilon$ for all $t \in [0, T]$. Clearly, $\eta_\epsilon \leq \epsilon$. Apart from this property, we also assume η_ϵ / ϵ converges to one as ϵ approaches zero.

c) Nearest Neighbor: Given a state x and a finite set V of states, the `Nearest` procedure returns the state in V that is closest to x, i.e., $\texttt{Nearest}(V, x) := \arg\min_{x' \in V} \|x' - x\|$.

Algorithm 1: The RRT* Algorithm

```
V ← {z_init}; E ← ∅; i ← 0;
while i < N do
    G ← (V, E);
    z_rand ← Sample(i); i ← i + 1;
    (V, E) ← Extend(G, z_rand);
```

Algorithm 2: The `Extend` Procedure

```
V' ← V; E' ← E;
z_nearest ← Nearest(G, z);
(x_new, u_new, T_new) ← Steer(z_nearest, z);
z_new ← x_new(T_new);
if ObstacleFree(x_new) then
    V' := V' ∪ {z_new};
    z_min ← z_nearest; c_min ← Cost(z_new);
    Z_nearby ← NearVertices(G, z_new, |V|);
    for all z_near ∈ Z_nearby do
        (x_near, u_near, T_near) ← Steer(z_near, z_new);
        if ObstacleFree(x_near) and x_near(T_near) = z_new
        then
            if Cost(z_near) + J(x_near) < c_min then
                c_min ← Cost(z_near) + J(x_near);
                z_min ← z_near;
    E' ← E' ∪ {(z_min, z_new)};
    for all z_near ∈ Z_nearby \ {z_min} do
        (x_near, u_near, T_near) ← Steer(z_new, z_near);
        if x_near(T_near) = z_near and ObstacleFree(x_near)
        and Cost(z_near) > Cost(z_new) + J(x_near) then
            z_parent ← Parent(z_near);
            E' ← E' \ {(z_parent, z_near)};
            E' ← E' ∪ {(z_new, z_near)};
return G' = (V', E')
```

d) Near Neighbors: The `Near` procedure returns a subset of V with states close to x in the following sense:

$$\texttt{Near}(V, x) := V \bigcap \mathrm{Box}^w\left(x, \gamma \left(\frac{\log |V|}{|V|}\right)^{1/D}\right),$$

where $|V|$ denotes the cardinality of V, D is the Hausdorff dimension of the distribution generated by the dynamics, and γ is a constant that is independent of $|V|$. Note at this point that the volume of the weighted box in the right hand side of the definition above is equal to $\gamma^D (\log |V| / |V|)$.

e) Collision Checking: Given a trajectory $x : [0, T] \to X$, the $\texttt{ObstacleFree}(x)$ procedure returns true if x avoids collision with obstacles, i.e., $x(t) \notin X_{\mathrm{obs}}$ for all $t \in [0, T]$, and returns false otherwise.

Let us remark that the sampling, local steering, and near neighbor procedures differ from their counterparts in RRT* for holonomic systems [9] in a number of ways. Firstly, the sampling procedure is assumed to return random samples from the maximal integral manifold through the initial state.[3] Second, the steering procedure must have the topological property[4] To guarantee optimality, in addition,

[3] If the Lie hull of the distribution generated by the dynamics spans the tangent space of the state space at every point of X, then the maximal integral manifold is X itself. Hence, in that case, the sampling procedure returns samples from the free space $X \setminus X_{\mathrm{obs}}$.

[4] This property is often required even when one is concerned only with finding a feasible trajectory and optimality is not a concern [17].

it requires that η_ϵ/ϵ converges to one as ϵ approaches zero. Roughly speaking, this implies that as ϵ approaches zero, the trajectories returned by the local steering algorithm resemble time-optimal trajectories. Third, and most important, the near neighbors are not computed considering an Euclidean ball, but within a weighted Euclidean box the shape of which resembles the shape of the sub-Riemannian ball.

The RRT* algorithm is given in Algorithm 1. The algorithm is the same as that presented in [9] on all accounts except the primitive procedures. If the Hausdorff dimension of the distribution is equal to that of the state space, i.e., $D = n$, that is, when the system at hand is holonomic, then Algorithm 1 reduces to the RRT* algorithm presented in [9].

V. Analysis

In this section, we analyze the proposed algorithm in terms of asymptotic optimality and computational complexity.

First, let us recall some definitions from [9] modified for the setting in this paper. Let δ be a positive real number. A state x is said to be in the δ-interior of the free space, if the closed ball of radius δ lies entirely inside $X_{\text{free}} = X \setminus X_{\text{obs}}$. The collection of all states that are in the δ-interior of X_{free}, denoted by $\text{int}_\delta(X_{\text{free}})$, is called the δ-interior of X_{free}.

A dynamically-feasible trajectory $x : [0, T] \to X$ is said to have *strong δ-clearance* if it lies entirely in the δ-interior of the free space, i.e., $x(t) \in \text{int}_\delta(X_{\text{free}})$ for all $t \in [0, T]$. A dynamically feasible trajectory is said to be *robustly feasible* it has strong δ-clearance, for some $\delta > 0$, and solves

Let Σ_T denote the set of all Lebesgue measurable functions from $[0, T]$ to $\mathbb{R}^n$. Given $x, x' \in \Sigma$, define $\|x' - x\|_\infty := \max_{t\in[0,T]} \|x'(t) - x(t)\|$, where $\|\cdot\|$ is the usual Euclidean norm on $\mathbb{R}^n$. A continuous function $\psi : [0, 1] \to \Sigma$ is called a *homotopy* between two trajectories $x, x' : [0, T] \to X_{\text{free}}$, if $\psi(0) = x$ and $\psi(1) = x'$ and $\psi(\tau)$ is collision-free for all $\tau \in [0, 1]$. The trajectories x and x' are said to be *homotopic*, if there exists a homotopy between them. A dynamically-feasible trajectory $x : [0, T] \to X$ is said to have *weak δ-clearance* if there exists a path $x' : [0, T] \to X$ that has strong δ-clearance, and there exists a homotopy ψ between x and x' such that $\psi(\tau)$ has strong δ_τ-clearance for some $\delta_\tau > 0$ for all $\tau \in (0, 1)$. The reader is referred to [9] for examples of trajectories with weak δ-clearance. A dynamically-feasible trajectory $x^* : [0, T] \to X$ that solves the optimal motion planning problem is said to be *robustly optimal* if it has weak δ-clearance and any sequence $\{x_n\}_{n\in\mathbb{N}}$ of trajectories that converge to x^* satisfies $\lim_{n\to\infty} c(x_n) = c(x^*)$.

A sampling-based algorithm is said to be *asymptotically optimal* if, for any instance of the motion planning problem that admits a robustly optimal solution with finite cost c^*, $\mathbb{P}(\limsup_{n\to\infty} Y_n = c^*) = 1$, where Y_n is the cost of the best path after invoking the sampling procedure n times.

Theorem 5 (Asymptotic Optimality) *The RRT* algorithm (Algorithm 1) is asymptotically optimal.*

Let M_n^{RRT} denote the number of simple operations performed the by the RRT algorithm in iteration n. The random variable $M_n^{\text{RRT}^*}$ is defined similarly.

Theorem 6 (Computational Complexity) *The RRT* and RRT algorithms have the same per-iteration asymptotic computational complexity, i.e., there exists a finite c such that* $\lim_{n\to\infty} \mathbb{E}[M_n^{\text{RRT}^*}]/\mathbb{E}[M_n^{\text{RRT}}] \leq c$.

The proofs of these theorems are omitted for the sake of brevity. The proof of Theorem 5 is the same as the corresponding result in our previous work in [9] with one exception: the balls with volume $(\log n/n)$ are replaced with scaled boxes (as defined in the presentation of the `Near` procedure), which also have volume $\log n/n$, where n is the number of vertices in the graph. The proof of Theorem 6 is also similar to the corresponding result in [9].

VI. Computational Experiments

The algorithm proposed in Section IV was implemented using the C++ programming language . The implementation was executed on a computational platform powered by a processor with 2.66 GHz clock speed and 8GB of RAM.

The algorithm was run in an empty environment of length 20 and width 20 centered at the origin. The cost function was chosen as the time to reach the goal region, a square region centered at $(7, 7)$ of size 2 in both directions.

The results are compared with a naive algorithm that is asymptotically optimal but not computationally efficient. This algorithm runs exactly as the RRT*, except the `Near` procedure is defined as follows: $\texttt{Near}(V, x) := \{x' \in X : \|x' - x\|_\infty \leq (\log n/n)^{1/D}\}$, where $\|\cdot\|_\infty$ denotes the L_∞ norm. Hence, this algorithm seeks connections within a hypercube, rather than a scaled box. It can be shown that this hypercube is large enough to ensure asymptotic optimality. In fact, it includes the scaled box in the earlier definition of the `Near` procedure. However, it makes too many connections.

In the experimental study, the proposed algorithm is compared with the naive algorithm in Monte-Carlo simulations where each algorithm is run 50 times independently. The results are shown in Figure 2. In Figure 2.(a), we compare the number of connections made by each algorithm. More precisely, the average number of connections per iterations is divided by $\log(n)$, where n is the number of iterations. From Theorem 6, we expect that this quantity is a constant for the proposed algorithm, since the number of connections should be order $\log n$, which can be seen in the plot. However, in the naive algorithm, the same quantity is clearly an increasing function of n. In fact, the excess number of connections lead to substantial computational overhead in the planning process as seen in Figure 2.(b), where we plot the average computation time to reach a particular iteration for both algorithms. Yet, most of the excess connection attempts are indeed unsuccessful. As seen from Figure 2.(c), the difference in the quality of the solution provided by the two algorithms is negligible, despite the substantial difference in computational costs.

Acknowledgements

This work was supported in part by the Army Research Office (ARO MURI award W911NF-11-1-0046) and the National Science Foundation (grant CNS-1016213).

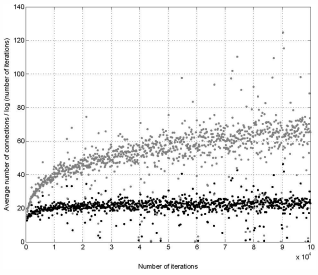

(a) Average number of connections over log of # of iterations vs. # of iterations.

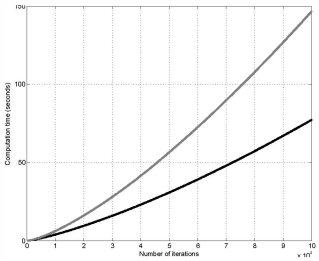

(b) Average time to reach a particular iteration.

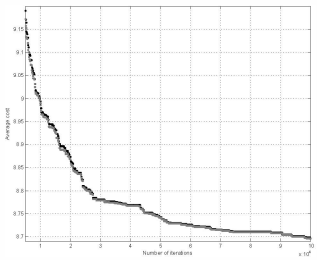

(c) Average cost versus the number of iterations.

Fig. 2. The two algorithms are compared in terms of the average number of connections (Fig a), the average time to reach a particular iteration (Fig c), and the average cost at a particular iteration (Fig b). The proposed approach is shown in black, and the naive algorithm is shown in grey.

VII. Conclusion

We have proposed an extension of the RRT* that can handle a large class of non-holonomic dynamical systems. The enabling idea behind this extension is to seek connections within a scaled box, the dimensions and the orientation of which is dictated by the ball-box theorem of sub-Riemannian geometry. We have shown that the proposed algorithm guarantees asymptotic optimality, without sacrificing computational efficiency. We have evaluated the proposed algorithm, in Monte-Carlo computational experiments, when compared to a naive algorithm that seeks connections in a hypercube large enough to guarantee asymptotic optimality. The results indicate that the proposed approach provides significant savings in computation time with almost no sacrifice in the quality of the solution, when compared to the naive solution.

References

[1] Steven Michael LaValle. *Planning algorithms*. Cambridge Univ Pr, May 2006.

[2] J. Latombe. Motion Planning: A Journey of Molecules, Digital Actors, and Other Artifacts. *International Journal of Robotics Research*, 18(11):1119–1128, 1999.

[3] J. Reif. Complexity of the Generalized Mover's Problem. In J Schwartz, J Hopcroft, and M. Sharir, editors, *Planning, Geometry, and Complexity of Robot Motion*, pages 267–281. Ablex Publishing Corp., 1987.

[4] L. Kavraki, P. Svestka, J. Latombe, and M. H. Overmars. Probabilistic roadmaps for path planning in high-dimensional configuration spaces. *IEEE Transactions on Robotics and Automation*, January 1996.

[5] S M LaValle and J Kuffner. Randomized kinodynamic planning. *The International Journal of Robotics Research*, 20(5):378–400, 2001.

[6] Y. Kuwata, J. Teo, G. Fiore, S. Karaman, E. Frazzoli, and J. P. How. Real-Time Motion Planning with Applications to Autonomous Urban Driving. *IEEE Transactions on Control Systems*, 17(5):1105–1118, 2009.

[7] C. Urmson and R. Simmons. Approaches for heuristically biasing RRT growth. In *Proceedings of the IEEE/RSJ International Conference on Intelligent Robots and Systems*, 2003.

[8] D. Furgeson and A. Stentz. Anytime RRTs. In *Proceedings of the IEEE/RSJ International Conference on Intelligent Robots and Systems*, 2006.

[9] S Karaman and E Frazzoli. Sampling-based Algorithms for Optimal Motion Planning. *International Journal of Robotics Research*, 30(7):846–894, 2011.

[10] S. Karaman, M. Walter, A. Perez, E. Frazzoli, and S. Teller. Anytime Motion Planning using the RRT*, In *IEEE International Conference on Robotics and Automation (ICRA)*, 2011.

[11] A. Perez, S. Karaman, M. Walter, A. Shkolnik, E. Frazzoli, and S. Teller. Asymptotically-optimal Path Planning for Manipulation using Incremental Sampling-based Algorithms. In *Proceedings of the IEEE/RSJ International Conference on Intelligent Robots and Systems (IROS)*, 2011.

[12] S. Karaman and E. Frazzoli. Optimal Kinodynamic Motion Planning using Incremental Sampling-based Methods. In *IEEE Conference on Decision and Control (CDC)*, Atlanta, GA, December 2010.

[13] A. Perez, R. Platt, G. Konidaris, L. Kaelbling, and T. Lozano-Perez. LQR-RRT*: Optimal sampling-based motion planning with automatically derived extension heuristics*: Optimal sampling-based motion planning with automatically derived extension heuristics. In *IEEE International Conference on Robotics and Automation*, 2012.

[14] D. J. Webb and J. van den Berg. Kinodynamic RRT*: Optimal motion planning for systems with linear differential constraints. arXiv, May 2012.

[15] H J Sussmann. A General Theorem on Local Controllability. *SIAM Journal of Control and Optimization*, 25(1):158–194, 1987.

[16] L E Dubins. On Curves of Minimal Length with a Constraint on Average Curvature, and with Prescribed Initial and Terminal Positions and Tangents. *American Journal of Mathematics*, 79(3):497–516, 1957.

[17] J P Laumond, S Sekhavat, and F Lamiraux. Guidelines in Nonholonomic Motion Planning for Mobile Robots. In *Robot Motion Planning and Control*, pages 171–253. Springer, 1998.

[18] R Montgomery. *A Tour of Subriemannian Geometries, Their Geodesics, and Applications*. American Mathematical Society, 2002.

[19] A Bellaiche. The Tangent Space in Sub-Riemannian Geometry. In A Bellaiche and J Risler, editors, *Sub-Reimannian Geometry*, pages 1–78. Birkhauser, 1996.

[20] M Gromov. Carnot-Caratheodory spaces seen from within. In *Sub-Riemannian Geometry*, pages 79–323. Birkhauser, 1996.

[21] R S Strichartz. Sub-Riemannian Geometry. *Journal of Differential Geometry*, 24:221–263, 1986.

[22] J R Munkres. *Topology*. Prentice Hall, 2nd edition, 2000.

[23] Jean-Claude Latombe. *Robot motion planning*. Springer, 1991.

[24] J A Reeds and L A Shepp. Optimal paths for a car that goes both forwards and backwards. *Pacific Journal of Mathematics*, 145(2):367–393, 1990.

[25] W L Chow. Uber Systeme von Linearen Partiellen Differentialglaichungen erster Ordnung. *Math. Ann.*, 117:98–105, 1970.

[26] F Bullo and A D Lewis. *Geometric Control of Mechanical Systems*. Springer, 2004.

[27] V Jurdevic. *Geometric Control Theory*. 1997.

[28] A Isidori. *Nonlinear Control Systems*. Springer, 3rd edition, 1994.

[29] L Hormander. Hypoelliptic second order differential equations. *Acta Mathematica*, 119(1):147–171, 1967.

[30] A Bellaiche, F Jean, and J J Risler. Geometry of Nonholonomic Systems. In J P Laumond, editor, *Robot Motion Planning and Control*, pages 55–91. Springer, 1998.

[31] R Hermann. On the accessibility problem in control theory. In *International Symposium on Nonlinear Differential Equations and Nonlinear Mechanics*, 1963.

[32] A J Krener. A Generalization of Chow's Theorem and The Bang-Bang Theorem To Nonlinear Control Problems. *SIAM Journal on Control*, 12(1):43–52, 1974.

[33] H Hermes. Lie Algebras of Vector Fields and Local Approximation of Attainable Sets. *SIAM Journal on Control and Optimization*, 16(5):715–727, 1978.